Arch. Biol. Sci., Belgrade, 64 (3), 943-951, 2012 DOI:10.2298/ABS1203943U

EFFECTS OF METHIMAZOLE-INDUCED HYPOTHYROIDISM ON IMMUNOHISTOCHEMICAL, STEREOMORPHOMETRIC AND SOME ULTRASTRUCTURAL CHARACTERISTICS OF PANCREATIC B-CELLS

MIRELA UKROPINA[1], RADMILA GLIŠIĆ[2], KSENIJA VELIČKOVIĆ[1], MILICA MARKELIĆ[1], I. GOLIĆ[1], MAJA ČAKIĆ-MILOŠEVIĆ[1] and VESNA KOKO[1,3]

[1] *University of Belgrade, Faculty of Biology, Institute of Zoology,* 11000 Belgrade, Serbia
[2] *University of Kragujevac, Faculty of Science,* 34000 Kragujevac, Serbia
[3] *University of Belgrade, Institute for Medical Research,* 11000 Belgrade, Serbia

Abstract – The function of pancreatic β-cells is to produce and secrete insulin, a crucial hormone in carbohydrate metabolism. The transcription factor PDX1 is required for insulin gene transcription and mature β-cell function. Since this factor is regulated by triiodothyronine, a disturbance in insulin biosynthesis and/or secretion is usually related to a deficiency of this hormone. In the present study, we used methods of immunohistochemistry, stereology and electron microscopy to explore the correlation between altered thyroid status and insulin synthesis/secretion in a model of methimazole-induced hypothyroidism in rats. In hypothyroid animals fewer functional PDX1-positive β-cells were detected in the islets of Langerhans, while insulin immunostaining was stronger. Stereological analysis of β-cell granules revealed more numerous immature insulin granules in hypothyroid rats. Taken together, these data suggest that the applied treatment caused impaired insulin synthesis and secretion. Rare cells with granules characteristic for both α- and β-cells observed in hypothyroid animals could provide functional compensation for diminished insulin synthesis.

Key words: Pancreas, hypothyroidism, PDX1, β-cell granules

INTRODUCTION

The pancreas is a gland with both endocrine and exocrine functions. Its endocrine function is based on the secretory action of several types of endocrine cells that cluster together to form the islets of Langerhans. The most numerous of these cells are β-cells that are responsible for insulin synthesis and secretion. Insulin has a key regulatory role in carbohydrate and lipid metabolism, in particular their storage and utilization (Saltiel and Kahn, 2001).

The primary stimulus for insulin secretion, but also for insulin gene transcription and insulin mRNA translation, is an increase in the blood glucose level (Permutt and Kipnis, 1972; Goodison et al., 1992). After insulin is synthesized on the rough endoplasmic reticulum and processed in the Golgi complex, it is packed in secretory granules, where further modification and final storage take place. At the molecular level, insulin gene expression is stimulated by transcription factors PDX1 (pancreatic and duodenal homeobox-1) and NeuroD1 (neurogenic differentiation 1), which are both necessary for maintaining mature β-cell function (Andrali et al., 2008; Kaneto et al., 2009). Many hormones, with thyroid hormone triiodothyronine (T3) among them, are involved in the positive regulation of these transcription factors (Campbell and Macfarlane, 2002; Lin and Sun, 2011).

In mammals, an altered thyroid status adversely affects many organs and tissues, including the pancreas (Lu et al., 1988; Lee et al., 1989). So far, published data considering the concentration of insulin in the blood in a common thyroid disorder such as hypothyroidism are surprisingly inconsistent and often contradictory. However, probably the most numerous are reports describing decreased insulin levels due to the negative regulation of its secretion from β-cells in the systemic hypothyroid state, (Katsilambros et al., 1972; Lenzen and Bailey, 1984; Gomez Dumm et al., 1985; Cortizo et al., 1985; Ramos et al., 1998, 2001).

Given this background, the aim of the present study was to illustrate and quantitatively demonstrate the correlation of insulin synthesis/secretion with thyroid hormone concentration in the milieu of their systemic deprivation, employing immunohistochemistry, electron microscopy and stereological methods.

MATERIALS AND METHODS

Animals and treatment

Male Wistar rats (*Rattus norvegicus*) 8 weeks in age and weighing 210 ± 35 g, were acclimated to 21±1°C and maintained under an intermittent 12 h periods of light and dark. Five days before the beginning of the experiment, the rats were individually housed into cages. They were divided into two groups, each consisting of 8 animals. The first group was the intact control and was given commercial rat food and water *ad libitum*. The rats from the second group had free access to both commercial rat food and a 0.02% (w/v) methimazole (2-mercapto-1-methyl-imidazole, MMI) (Sigma-Aldrich, St. Louis, MO) solution in tap water. Food and fluid input were monitored during the experiment, for three weeks.

At the end of the experiment, the rats were weighed and decapitated using a guillotine (Harvard Apparatus, Holliston, MA). The pancreas was quickly excised, freed of fat tissue on ice and weighed. Relative pancreatic mass was expressed as a percentage of the body mass (BM). Blood was collected from the trunk after decapitation. Animal handling and treatment were carried out in accordance with the Serbian Laboratory Animal Protection Law proposed guidelines and protocols, approved by the Ethical Committee of Faculty of Biology, University of Belgrade.

Insulin, total triiodothyronine (T3) and total thyroxin (T4) serum levels were measured by the RIA method (INEP, Zemun, Serbia).

Light microscopy

Pancreases were fixed in 10% (v/v) neutral buffered formalin. After fixation, each pancreas was cut into eight uniform pieces. Four pieces were selected in a systematic random manner (Gundersen and Jensen, 1987). The samples taken from each animal were dehydrated in an ascending concentration of alcohol, cleared in xylol and embedded in paraplast. From each block of pancreas, 5 μm thick sections were obtained, using a Reichert rotation microtome.

For identifying the presence of dead cells, sections were incubated in 1 mg/ml propidium iodide solution in water for 10 min. Propidium iodide binds to the nuclei in all cells because we are dealing with fixed tissue. However, apoptotic cells have condensed nuclei, as opposed to heterochromatin staining in living cells at the moment of fixation. Sections were observed on a fluorescence microscope Zeiss Observer.Z1 and images taken using the AxioCamMR3 and AxioVision Rel4.7 software.

Immunohistochemistry

For identification of β-cells, immunohistochemistry was performed using the labeled streptavidin biotin (LSAB) method. The sections were incubated with antiserum against insulin (polyclonal guinea pig anti-insulin A0564, Dako, 1:500). Incubation with a primary antibody was performed at room temperature for 60 min.

To demonstrate cells in active phases of the cell cycle, the mouse monoclonal Ki-67 antibody was

used (M7248, DakoCytomation, 1:30). Before 30 min incubation with primary antibody at room temperature, heat-induced epitope retrieval was performed (20 min. in 10mM citrate buffer pH 6).

Immunostaining with primary anti-PDX1 antibody (rabbit polyclonal ab47267, Abcam, 1:750) was performed on chosen sections (overnight incubation, 4°C).

All primary antibody incubations were preceded by specimen incubation in 3% hydrogen peroxide and protein block, followed by sequential incubations with a biotinylated antibody and peroxidase-labeled streptavidin. Staining was completed after incubation in a DAB+chromogen solution (Mouse and Rabbit Specific HRP/DAB detection IHC kit, ab64264, Abcam). The nuclei were counterstained with Mayer's hematoxylin.

All immunostained sections were analyzed on a Leica DMRB Photo Microscope and photographs were taken using a JVC TK 1280E Video Camera (Leica) and the QWin program (Leica).

Electron microscopy

After short fixation in 10% (v/v) neutral buffered formalin and washing by three changes of phosphate buffer (one change daily), tissue samples of the pancreas from each group were cut into small blocks (approx. 1 mm^3) and immersed in 2.5% glutaraldehyde in 0.1 M phosphate buffer (pH-7.4) for 60 min. All specimens were post-fixed for 1 h in 1% osmium tetroxide in the same buffer, dehydrated in a series of increasing ethanol concentrations and propylene-oxide, and embedded in Araldite. Ultrathin sections were obtained using a Leica EM UC6 ultramicrotome, contrasted with uranyl acetate and lead citrate, and examined under a Philips CM 12 electron microscope. Electron micrographs of β-cells enabled us to precisely determine the number of granules per unit area, using Image J 1.45 software. These images also served for the assessment of mature vs. immature granules ratio.

Stereological analysis

Stereological analysis of islets and their insulin-producing cells were performed by a 'point counting' technique, using Weibel's multipurpose test grid M 42 (Weibel et al., 1966). Conventional morphometry and standard stereological equations were used to calculate the following parameters: islet diameter, volume and numerical density of islets, number of islets per unit area, total number of islets, and islet mass; volume density of β-cells, β-cell mass, profile area of a single endocrine cell and number of β-cells per islet.

With a graticule of a calibrated linear scale, the major (a) and minor (b), and axes of the islets at a right angle to (a), were measured and the mean islet diameter was calculated. The relative volume (volume density or V_v) of the islets was calculated by dividing the number of points over the islets by the number of points over the total tissue section. The number of islets per unit area (numerical area density or N_A) was determined by the formula $N_A = N/A_T$, where N is the number of sectioned profiles of islets and A_T the area of the section. The equation $A_T = P_t \times \sqrt{3}/2 \times d^2$ was used to determine the area of the section, where P_t is the number of hits over the section and d is the test line. The numerical density of islets (N_v) was determined using the method of DeHoff and Rhines as described by Aherne and Dunnill (1982a): $N_v = k/\beta \times \sqrt{N_A^3/V_v}$, where $k/\beta = 1.485$, the constant value for a sphere. The absolute (total) number of islets was obtained by multiplying the numerical density of the islets by the pancreatic volume, which was determined according to Aherne and Dunnill (1982b) from the formula V (ml) = 0.95 x W (g), where W is pancreatic weight. Islet mass was calculated by multiplying the islet volume density by pancreas weight.

The relative volume (volume density, V_v) of β-cells in the islets of Langerhans was calculated by dividing the number of points over immunohistochemically stained β-cells by the number of points over the islets. The mass of β-cells was determined by multiplying the volume density of β-cells by the pancreas weight. The profile area of the β-cell was also estimat-

Table 1. Effects of MMI treatment on the rat body and pancreatic masses, daily food and fluid intake, and some biochemical parameters in serum. Values are means ± SEM of eight animals.

	Control	Methimazole	p value
Initial body mass (g)	217.5 ± 9.6	218.0 ± 7.4	n.s.
Final body mass (g)	352.7 ± 9.5	293 ± 5.9	< 0.001
Body mass gain (g)	135.2 ± 1.8	75.0 ± 6.8	< 0.001
Average daily food intake (g)	28.36 ± 0.62	22.63 ± 0.56	< 0.001
Average daily fluid intake (ml)	42.45 ± 1.20	33.58 ± 1.58	< 0.05
Pancreatic mass (g)	1.11 ± 0.05	0.82 ± 0.02	< 0.001
Relative pancreatic mass (g/100g BM)	0.314 ± 0.015	0.279 ± 0.006	n.s.
Insulin (mIU/l)	90.72 ± 11.42	68.30 ± 5.17	n.s.
T3 (nmol/l)	1.23 ± 0.10	0.97 ± 0.06	< 0.05
T4 (nmol/l)	88.50 ± 3.07	3.42 ± 0.56	< 0.001

ed on the immunohistochemically stained sections of pancreas. This was obtained by dividing the total profile area of the β-cells by the total number of cells. The equation $A_T = P_t \times \sqrt{3}/2 \times d^2$ was used to determine the area of endocrine cells in individual islets of Langerhans, where A_T is the total β-cell area, P_t is number of hits on β-cells and d is the test line. The number of β-cells per islet was obtained by dividing the number of β-cells over the number of islets.

Statistics

Values are presented as means ± standard error of mean (SEM). Student's *t*- test was used for statistical analysis; p values < 0.05 were regarded as being statistically significant.

RESULTS

Applied MMI treatment induced systemic hypothyroidism, which was confirmed by the decreased levels of both serum T3 and T4 (Table 1). This resulted in growth retardation, manifested by a significantly decreased body weight gain. The absolute and relative pancreatic masses were also decreased, although the reduction in relative mass was not statistically significant. The serum insulin level was decreased, but without statistical significance.

During the experiment, lower food and fluid intake were recorded in the MMI-treated animals (Table 1).

Histology and immunohistochemistry

Under light microscopy, differences between the groups in the general histological appearance of the Langerhans islets were not observed. Immunohistochemically stained β-cells were located in the central portion of the Langerhans islets. However, the immunopositive reaction appeared to be more intense in the hypothyroid animals (Fig. 1).

Immunolabeling of PDX1-positive cells showed a clear difference in the expression of this nuclear protein between the groups (Figs. 2a and b). In the control group, numerous immunopositive nuclei were distributed predominantly in the central part of the islets, while in the MMI-treated animals a weak reaction was rarely observed.

Cell proliferation was assessed on Ki67 immunohistochemically labeled tissue. In the control rats, immunopositive cells were scattered throughout the central portion of the islet (Fig. 3a). In the MMI-treated animals, however, rare Ki67 positivity was observed at the islet periphery, while it was ab-

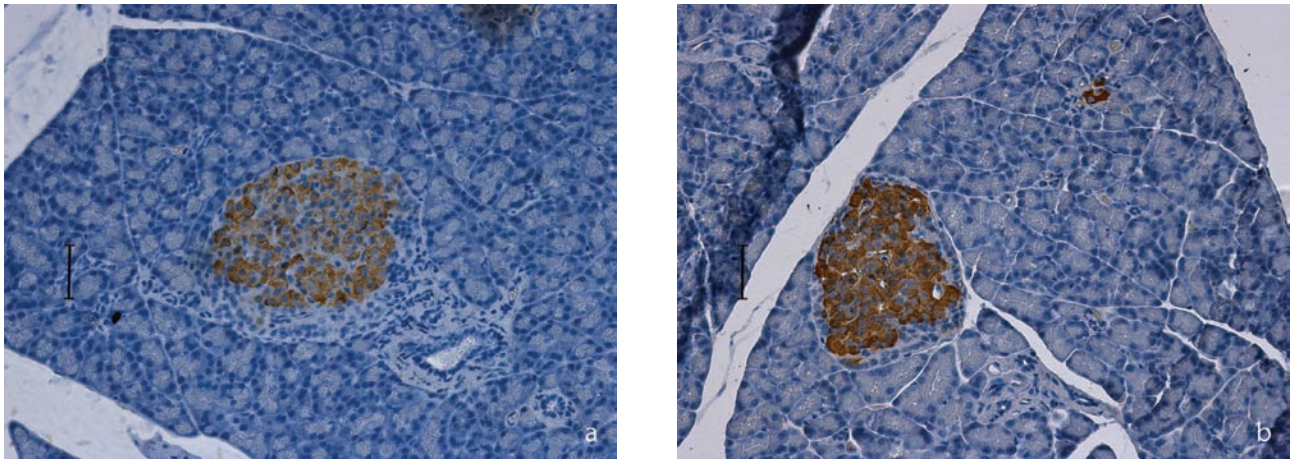

Fig. 1. Insulin containing β-cells occupy the central portion of the islets, and display moderately strong staining in control rats (a) and intense reaction in methimazole treated rats (b). (bar=50μm)

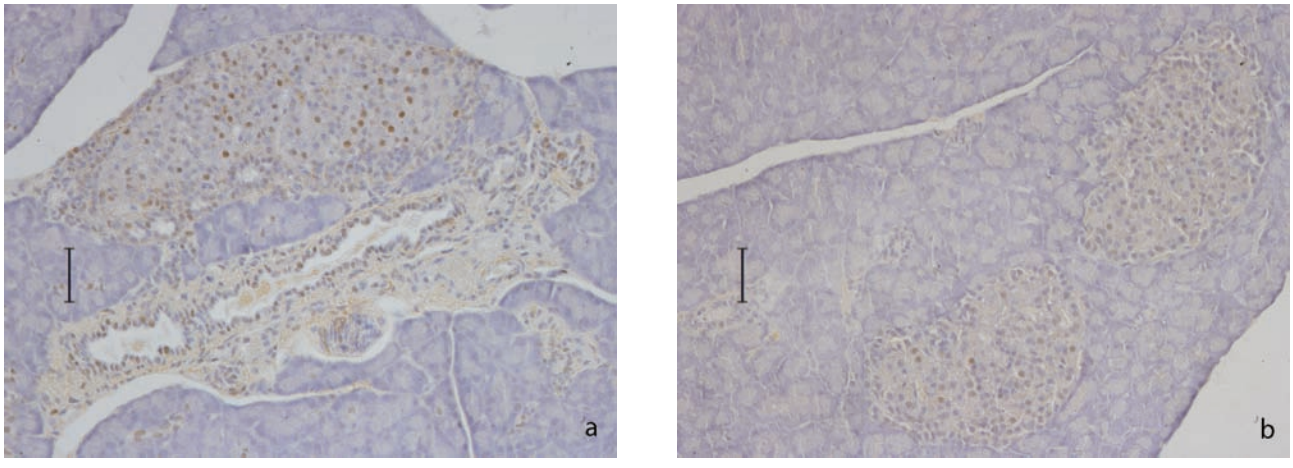

Fig. 2. Strong PDX1 immunopositivity is evident in the central portion of the islet of Langerhans in control pancreas (a). In hypothyroid pancreas (b) weaker reaction is present in a few centrally placed islet cells. (bar=50μm)

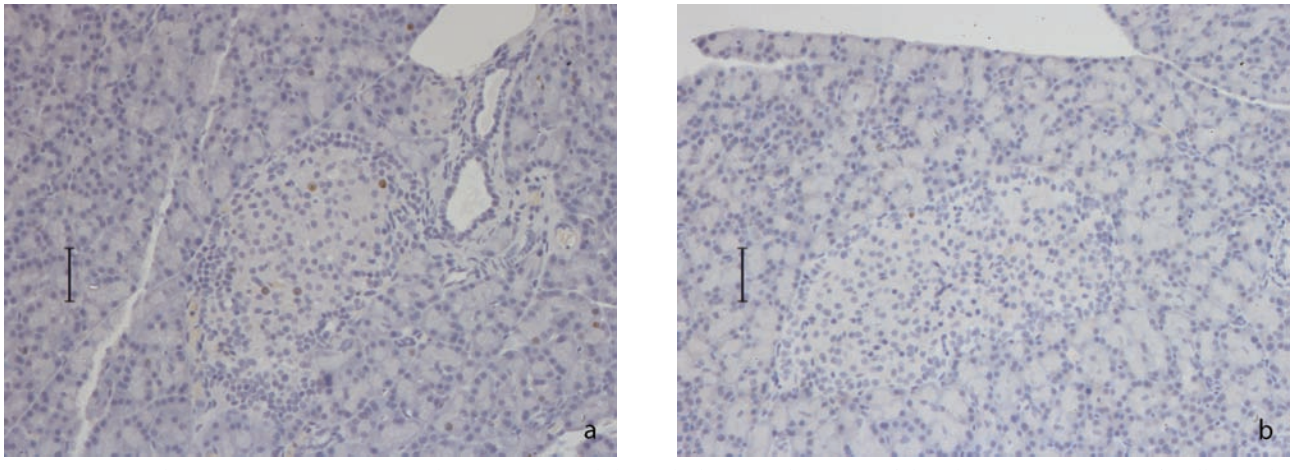

Fig. 3. In control pancreas Ki67-positive nuclei were scattered through the central portion of the islet (a). Ki67 positive β-cells are absent in islet of methimazole treated rats (b). Immunopositivity is present in scarce peripherally placed cells, corresponding to α-cells. (bar=50μm)

Table 2. Results of stereological investigation of pancreatic islets in control and methimazole treated rats. Values are means ± SEM of eight animals.

	Control	Methimazole	p value
Absolute volume of pancreas (ml)	1.05 ± 0.049	0.78 ± 0.021	<0.001
V_v of islets (mm^0)	0.012 ± 0.0027	0.016 ± 0.0022	n.s.
N_A (number of islets per mm^2)	0.73 ± 0.12	1.19 ± 0.13	<0.05
N_v (number of islets per cm^3)	8919 ± 1686	16214 ± 2069	<0.05
Absolute number of islets	9188 ± 1655	12489 ± 1423	n.s.
Mean islet diameter (μm)	135 ± 15.9	125 ± 8.1	n.s.
Islet mass (mg)	12.9 ± 2.6	13.4 ± 1.9	n.s.

sent among the cells that positionally correspond to β-cells (Fig. 3b).

The propidium iodide-stained pancreas revealed sporadic homogenous, bright red apoptotic nuclei in both the control and hypothyroid group (not shown).

Stereological results

The results of stereological investigation of the pancreatic islets are presented in Table 2. Since the absolute pancreas volume was reduced after MMI treatment while the islet number, mass and mean islet diameter were unchanged, the number of pancreatic islets per unit area and per unit volume consequently increased. However, the decrease in pancreas size was not sufficient to significantly affect the islets' volume density.

Quantitative analysis of β-cells (Table 3) showed that the profile area of a single β-cell was significantly decreased, while other parameters (β-cells' volume density, mass and number per islet) remained unchanged.

The β-cell granules are membrane-bound spherical vesicles containing a dense core, surrounded by an electron-lucent halo. Electron microscopic study of β-cell granules revealed that in comparison to the control, the granules in the MMI-treated group were closely packed and more often possessed a circular

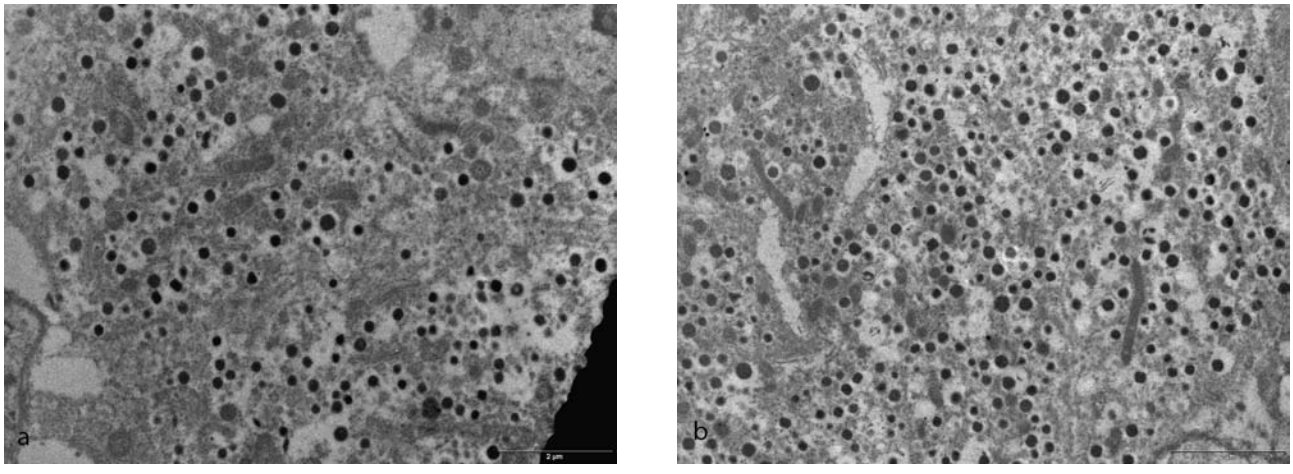

Fig. 4. Granules with square dense core are evident throughout the control β-cell (a). Typical β-cell from methimazole treated rats contains more numerous tightly packed granules with round dense core (b). (Orig. magn. x 8800)

Table 3. Results of stereological investigation of β-cells in control and methimazole treated rats. Values are means ± SEM of eight animals.

	Control	Methimazole	p value
V_v of β-cells (mm^0)	0.79 ± 0.034	0.73 ± 0.026	n.s.
β-cells mass (mg)	13.4 ± 3.3	12.4 ± 2.1	n.s.
Number of β-cells per islet	25.6 ± 4.08	32.5 ± 4.50	n.s.
Profile area of single β-cell (μm^2)	299.2 ± 24.7	202.8 ± 8.1	<0.01
Number of granules per 100 μm^2	194 ± 14.90	398 ± 63.17	< 0.01
Granules with circular core (%)	77 ± 1.37	96 ± 1.07	< 0.001
Granules with angular core (%)	23 ± 1.37	4 ± 1.07	< 0.001

instead of angular dense core, which is considered as sign of immaturity (Dodson and Steiner, 1998) (Figs. 4a and b). Indeed, a detailed stereological analysis of the electron micrographs showed a significant increase in the number of granules per unit area in the MMI-treated animals. In addition, the percentage ratio in this group was in favor of immature granules (Table 3).

In the MMI-treated animals, ultrastructural observation revealed within the islets the existence of individual α-like cells that, like the cell-specific granules, also contained those resembling β-cell granules (Fig. 5).

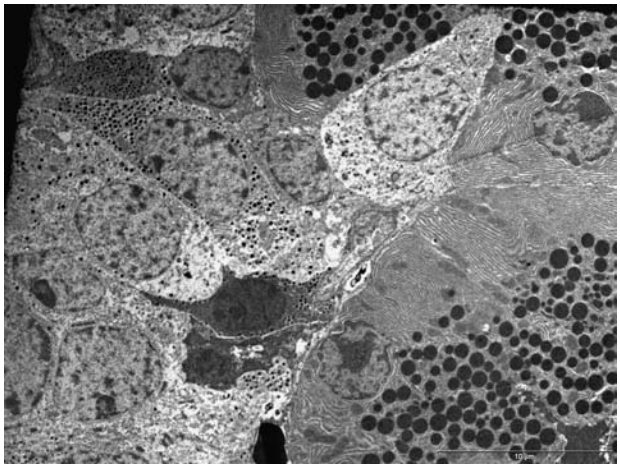

Fig. 5. In methimazole treated animals, at the islet periphery where majority of cells are of α type, peculiar cell is visible (top left): cytoplasm at its upper end is filled with typical dark α-cell granules, but below the nucleus granules possess wider halo, which is the hallmark of β-cell granules. (Orig. magn. x 2650)

DISCUSSION

To investigate the effects of systemic hypothyroidism on the immunohistochemical, stereomorphometric and some ultrastructural characteristics of pancreatic β-cells, we used an experimental model in which hypothyroidism was induced in rats by the antithyroid drug methimazole provided in drinking water, at a concentration of 0.02%, during 3 weeks. This treatment is conventionally used for establishing a hypothyroid state (Cooper et al., 1984; Petrovic et al., 2001), and its efficacy in this experiment was demonstrated by a significant decrease in both thyroid hormone serum levels.

The most remarkable effect of systemic hypothyroidism at the level of the whole organism was the significant lowering of body mass gain in the MMI-treated rats during the experiment. It is well known that a lack of thyroid hormones negatively affects all metabolic processes in the body, exerting an especially strong influence on protein synthesis (Tata et al., 1963; Tapley, 1964). At the same time, due to reduced energy expenditure, requirements for food and fluid consumption were also decreased, resulting in the reduced gain in body mass gain noted in this study.

Our results show that pancreatic mass was significantly lower in hypothyroid animals, but without changes in size, i. e. mass, diameter and number of its endocrine component. This indicates that the decrease in pancreatic mass is related entirely to the

reduction of its exocrine component. The unchanged relative pancreatic mass indicates that the reduction in the mass of the pancreas took place in parallel with body mass reduction and could be caused by a general growth cessation.

The results of our stereological analysis revealed that the relevant quantitative parameters for Langerhans islets, such as the volume density (V_v), total number, mean diameter and mass, remained unaltered in the pancreas of hypothyroid rats. At the same time, neither remarkable changes in cell death nor proliferation were demonstrated in slides stained with propidium iodide and immunostained for the proliferative marker Ki67, respectively. Taken together, these findings suggest that the applied treatment did not seriously affect the balanced turnover of β-cell population, leaving it relatively stable, as is the case in a normal adult pancreas (Ackermann and Gannon, 2007). Namely, during adulthood β-cells are a slowly renewing population, possessing steady and low rates of proliferation and apoptosis. Even when β-cell mass expands in line with an age-related increase in body weight, it is the result of an increase in individual cell size, rather than increasing proliferation (Montanya et al., 2000). Given that the absolute pancreas mass and volume were significantly reduced, the increase in numerical area density (N_A) and numerical density (N_V) of islets was to be expected. Despite this, there was no significant change in the volume density (V_V) of the islets, although it slightly increased. Since the pancreas can be considered to be a relatively quiescent organ in response to altered metabolic conditions (Bonner-Weir et al., 1993), this finding could be explained by an insufficient duration of the treatment.

Despite the overall stability of the β-cell population, stereological analysis unequivocally suggests a cessation in both the synthesis and release of insulin. The ultrastructural appearance of β-cell granules suggests an interruption in insulin secretion, since granules were more numerous in the cytoplasm of β-cells from the MMI-treated rats. Moreover, immature granules with a circular dense core were detected in a significantly greater percentage in this group. Insulin gene expression is under the direct positive control of the PDX1 transcription factor, which is in turn positively controlled by T3 (Campbell and Macfarlane, 2002; Andrali et al., 2008). The dramatic drop in PDX1-positive cells, which we observed in the islets of MMI-treated rats, is in accordance with this regulatory mode.

Electron microscopical observations revealed the existence of several cells that, according to most ultrastructural features, corresponded to glucagon-producing α-cells. However, in the cytoplasm of these cells, typical insulin-like granules were visible, clustered together in a precisely defined area (Fig. 5). It is known from a previous report by Chung and Levine (2010) that α-cells possess the capacity to co-express insulin and glucagon. In our opinion, in MMI-treated rats these glucagon/insulin co-expressing cells provide certain compensation for the deficient insulin-producing/secreting role of β-cells. The absence of a statistically significant decrease in the insulin concentration in the sera of hypothyroid rats could be explained, at least in part, by the secretory activity of these cells.

In conclusion, systemic hypothyroidism induced by MMI affects the endocrine pancreas, primarily by altering the ultrastructure and thus the function of its β-cell population. Newly emerged glucagon/insulin co-expressing α-like cells provide a nearly normal level of insulin in the circulation, thus compensating for the suppressed ability of β-cells to produce and/or release insulin.

REFERENCES

Ackermann, A.M. and *M. Gannon (2007). Molecular regulation of pancreatic beta-cell mass development, maintenance, and expansion. J. Mol. Endocrinol.* **38***, 193-206.*

Aherne, W.A. and *M.S. Dunnill* (1982a). Methods of counting discrete objects. In: *Morphometry*. (Eds. Aherne W.A., Dunnill M.S.), 60-74. Edward Arnold, London.

Aherne, W.A. and *M.S. Dunnill* (1982b). The estimation of whole organ volume. In: *Morphometry*. (Eds. Aherne W.A., Dunnill M.S.), 10-18. Edward Arnold, London.

Andrali, S.S., Sampley, M.L., Vanderford, N.L. and *S. Ozcan* (2008). Glucose regulation of insulin gene expression in pancreatic beta-cells. *Biochem. J.* **415**, 1-10.

Bonner-Weir, S., Baxter, L.A., Schuppin, G.T. and *F.E. Smith* (1993). A second pathway for regeneration of adult exocrine and endocrine pancreas. A possible recapitulation of embryonic development. *Diabetes* **42**, 1715-1720.

Campbell, S.C. and *W.M. Macfarlane* (2002). Regulation of the pdx1 gene promoter in pancreatic beta-cells. *Biochem. Biophys. Res.* **299**, 277-284.

Chung, C.H. and *F. Levine* (2010). Adult pancreatic alpha-cells: a new source of cells for beta-cell regeneration. *Rev. Diabet. Stud.* **7**, 124-131.

Cooper, D.S., Kieffer, J.D., Saxe, V., Mover, H., Maloof, F. and *E.C. Ridgway* (1984). Methimazole pharmacology in the rat: studies using a newly developed radioimmunoassay for methimazole. *Endocrinology* **114**, 786-793.

Cortizo, A.M., Gomez Dumm, C.L. and *J.J. Gagliardino* (1985). Effect of thyroid hormone levels upon pancreatic islet function. *Acta. Physiol. Pharmacol. Latinoam.* **35**, 181-191.

Dodson, G., and *D. Steiner* (1998). The role of assembly in insulin's biosynthesis. *Curr. Opin. Struct. Biol.* **8**, 189-194.

Gomez Dumm, C.L., Cortizo, A.M. and *J.J. Gagliardino* (1985). Morphological and functional changes in several endocrine glands induced by hypothyroidism in the rat. *Acta. Anat. (Basel)* **124**, 81-87.

Goodison, S., Kenna, S. and *S. J. Ashcroft* (1992). Control of insulin gene expression by glucose. *Biochem. J.* **285**, 563–568.

Gundersen, H.J. and *E.B. Jensen* (1987). The efficiency of systematic sampling in stereology and its prediction. *J Microsc.* 147, 229-263.

Kaneto, H., Matsuoka, T.A., Katakami, N. and *M. Matsuhisa* (2009). Combination of MafA, PDX-1 and NeuroD is a useful tool to efficiently induce insulin-producing surrogate beta-cells. *Curr. Med. Chem.* **16**, 3144–3151.

Katsilambros, N., Ziegler, R., Schatz, H., Hinz, M., Maier, V. and *E. F. Pfeiffer* (1972). Intravenous glucose tolerance and insulin secretion in the rat after thyroidectomy. *Horm. Metab. Res.* **4**, 377-379.

Lee, J.T., Lebenthal, E. and *P.C. Lee* (1989). Rat pancreatic nuclear thyroid hormone receptor: characterization and postnatal development. *Gastroenterology* **96**, 1151-1157.

Lenzen, S. and *C.J. Bailey* (1984).Thyroid hormones, gonadal and adrenocortical steroids and the function of the islets of Langerhans. *Endocr. Rev.* **5**, 411–421.

Lin, Y. and *Z. Sun* (2011). Thyroid hormone potentiates insulin signaling and attenuates hyperglycemia and insulin resistance in a mouse model of type 2 diabetes. *Br. J. Pharmacol.* **162**, 597-610.

Lu, R.B., Chaichanwatanakul, K., Lin, C.H., Lebenthal, E. and *P.C. Lee* (*1988).* Thyroxine effect on exocrine pancreatic development in rats. *Am. J. Physiol.* **254**, *G315*-321.

Montanya, E., Nacher, V., Biarnes, M. and *J. Soler* (2000). Linear correlation between beta-cell mass and body weight throughout the lifespan in Lewis rats: role of beta-cell hyperplasia and hypertrophy. *Diabetes* **49**, 1341–1346.

Permutt, M. A. and *D. M. Kipnis* (1972). Insulin biosynthesis. I. On the mechanism of glucose stimulation. *J. Biol. Chem.* **247**, 1194–1199.

Petrovic, N., Cvijic, G. and *V. Davidovic* (2001). The activity of antioxidant enzymes and the content of uncoupling protein-1 in the brown adipose tissue of hypothyroid rats: comparison with effects of iopanoic acid. *Physiol. Res.* **50**, 289-297.

Ramos, S., Goya, L., Alvarez, C. and *A.M. Pascual-Leone* (1998). Mechanism of hypothyroidism action on insulin-like growth factor -I and -II from neonatal to adult rats: insulin mediates thyroid hormone effects in the neonatal period. *Endocrinology* **139**, 4782–4792.

Ramos, S., Goya, L., Alvarez, C., Martın, M.A. and *A.M. Pascual-Leone* (2001). Effect of thyroxine administration on the IGF/IGF binding protein system in neonatal and adult thyroidectomized rats. *J. Endocrinol.* **169**, 111–122.

Saltiel, A.R. and *C.R. Kahn* (2001). Insulin signalling and the regulation of glucose and lipid metabolism. *Nature* **414**, 799–806.

Tapley, D.F. (1964). Mode and site of action of thyroxine. *Mayo Clin. Proc.* **39**, 626-636.

Tata, J.R., Ernster, L., Lindberg, O., Arrhenius, E., Pederson, S. and *R. Hedman* (1963). The action of thyroid hormones at the cell level. *Biochem. J.* **86**, 408–428.

Weibel, E.R., Kistler, G.S. and *W.A. Scherle* (1966). Practical stereological methods for morphometric cytology. *J.Cell Biol*, 30, 23-38.